Steering molecular organization and host–guest interactions using two-dimensional nanoporous coordination systems

SEBASTIAN STEPANOW[1], MAGALÍ LINGENFELDER[1], ALEXANDRE DMITRIEV[1], HANNES SPILLMANN[1], ERIK DELVIGNE[2], NIAN LIN*[1], XIAOBIN DENG[3], CHENGZHI CAI[3], JOHANNES V. BARTH*[2,4] AND KLAUS KERN[1,2]

[1]Max-Planck-Institut für Festkörperforschung, Heisenbergstrasse 1, D-70569 Stuttgart, Germany
[2]Institut de Physique des Nanostructures, Ecole Polytechnique Fédérale de Lausanne, CH-1015 Lausanne, Switzerland
[3]Department of Chemistry and Center for Materials Chemistry, University of Houston, Houston, Texas 77204-5003, USA
[4]Advanced Materials and Process Engineering Laboratory, University of British Columbia, Vancouver, British Columbia V6T 1Z4, Canada
*e-mail: N.Lin@fkf.mpg.de; johannes.barth@epfl.ch

Published online: 7 March 2004; doi:10.1038/nmat1088

Metal–organic coordination networks (MOCNs) have attracted wide interest because they provide a novel route towards porous materials that may find applications in molecular recognition, catalysis, gas storage and separation[1,2]. The so-called rational design principle—synthesis of materials with predictable structures and properties—has been explored using appropriate organic molecular linkers connecting to metal nodes to control pore size and functionality of open coordination networks[3–9]. Here we demonstrate the fabrication of surface-supported MOCNs comprising tailored pore sizes and chemical functionality by the modular assembly of polytopic organic carboxylate linker molecules and iron atoms on a Cu(100) surface under ultra-high-vacuum conditions. These arrays provide versatile templates for the handling and organization of functional species at the nanoscale, as is demonstrated by their use to accommodate C_{60} guest molecules. Temperature-controlled studies reveal, at the single-molecule level, how pore size and chemical functionality determine the host–guest interactions.

Transition metal carboxylates are widely used as constituents for nanoporous supramolecular materials[8,10–14]. The linker molecules used for the present study are 1,4-dicarboxylic benzoic acid (terephthalic acid, TPA), 1,2,4-tricarboxylic benzoic acid (trimellitic acid, TMLA) and 4,1′,4′,1″-terphenyl-1,4″-dicarboxylic acid (TDA), as depicted in Fig. 1. Our previous studies revealed that on deposition on a Cu(100) surface at room temperature, such species readily undergo complexation with coadsorbed Fe[10,15,16]. In particular, on the engagement of the endgroups in Fe-carboxylate formation, the linear linkages allow for the construction of MOCNs comprising surface-supported nanometre-size cavities with specific topology. They represent two-dimensional (2D) analogues to previously described 3D porous metal–organic framework structures[3–9]. The different backbone length (~7 Å for TPA and TMLA; ~15 Å for TDA) controls the cavity dimensions, whereas the additional side group of TMLA bestows a specific chemical functionality to the cavities.

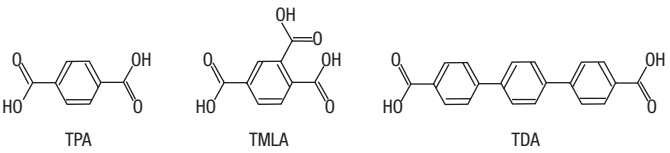

Figure 1 The linker molecules used in this study.

The tuning of 2D metal–organic networks using Fe and TPA or TDA is demonstrated by the scanning tunnelling microscopy (STM) data reproduced in Fig. 2. The identification of the organic molecules and Fe atoms in the MOCNs is based on a thorough analysis of carboxylate nanostructures from related benzoic acids and transition metal atoms at Cu(100)[10,15,16]. Their symmetry and shape is induced by the atomic arrangement of the underlying Cu atomic lattice, which induces the orientation along the principal directions of the substrate. The positioning of the flat-lying molecular species and the bonding of Fe atoms to their functional groups gives rise to networks comprising nanocavities of distinct shape and size.

The overview image in Fig. 2a shows the mesoscopic ordering of Fe-TPA MOCNs in domains extending up to 50 nm. In the high-resolution data in Fig. 2b,c, the formation of ladder-type and fully 2D interconnected networks is shown, the formation of which is controlled by the amount and ratio of the materials deposited (a complete account of the system is given elsewhere[17]). With the Fe concentration kept small, ladder-type structures with elongated cavities evolve (Fig. 2b). In such cases, not all carboxylate groups can participate in coordinating Fe atoms; presumably they form hydrogen-bridges (marked by dotted lines in Fig. 2b) with adjacent phenyl rings to stabilize the network structures further. On complete 2D Fe-carboxylate reticulation, a trellis

©2004 Nature Publishing Group

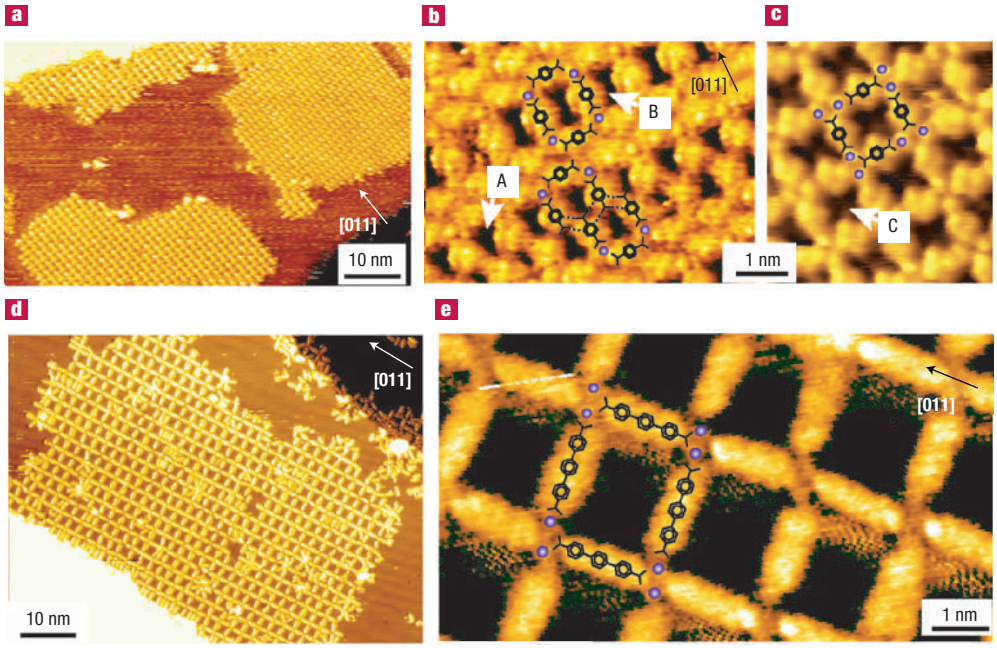

Figure 2 Tuning size and topology of nanocavities in metal–organic coordination networks on Cu(100). a, Overview STM image of large extended regular domains formed by TPA-Fe coordination networks. **b**, High-resolution image of ladder-type structures with two distinct types of nanocavities (marked by A and B), where not all available carboxylate groups are involved in coordination bonding. Potential intermolecular hydrogen-bridges are indicated by dashed lines. **c**, Fully interconnected network with complete 2D reticulation, giving rise to square cavities (marked by C). **d**, Topography of extended regular Fe-TDA trellis. **e**, High-resolution image of 2D reticulated Fe-TDA open network with rectangular nanocavities. Arrows on the images indicate the high-symmetry [011] direction of the Cu(100) substrate; positioning of molecular backbone and ligands are marked; Fe atoms are shown as blue spheres.

with a square unit cell and a cross-shaped cavity evolves, as shown in Fig. 2c (simultaneously with this phase a structural isomer with rectangular unit cell is formed). Earlier investigations revealed that TMLA and Fe assemble in MOCNs of almost identical topology as Fe-TPA MOCNs[10], which implies that the side groups at the ortho position of the TMLA molecules do not participate in the network formation. Instead, they modify the chemical properties of the pores, that is, the nanocavities of Fe-TPA MOCNs are enclosed by non-polar aromatic rings, whereas the rims of Fe-TMLA MOCNs comprise a highly reactive moiety.

The TDA molecule can be similarly used to construct 2D MOCNs that can be regarded as a higher analogue to the networks obtained with TPA or TMLA. This is demonstrated by the STM data in Fig. 2d,e, clearly revealing the reticulation of the components in an extended network with large cavities reflecting the increased length of the linker molecule used. It is easy to recognize how the TDA functional endgroups are pointing to the network intersections where metal–ligand interactions are operative. Again, there is mesoscopic order in the 50-nm range and the trellis orientation follows the principal substrate directions.

All obtained MOCNs were found to be robust, with their morphology being maintained up to a temperature of 500 K. Furthermore, they comprise open spaces that expose the Cu substrate. The cavities in the Fe-TPA and Fe-TMLA MOCNs are of the dimension of a small molecule (for example, ~5 Å × 5 Å for the type-C phase), whereas the Fe-TDA MOCNs provide large rectangular cavities extending to the nanometre range (~20 Å × 15 Å). The present approach therefore provides an elegant means to deliberately divide up a surface at the molecular scale[10,18]. As the chemical properties of the cavities are furthermore expected to depend on both the linker molecules (aromatic backbones and side groups) and node atoms, they can be regarded as nanoscale hosts providing a well-defined local chemical environment.

The simplest way to test the suitability of the engineered 2D MOCNs for organisation of functional materials and host–guest chemistry is to study their structural stability and steering effects in the coadsorption of nanoscale objects. As a trial species, C_{60} molecules were chosen, which can be easily brought to the surface. Controlling C_{60}–surface interactions and positioning is of both scientific and technological interest[18–21]. The STM images in Fig. 3 demonstrate that the cavities of the Fe-TPA MOCNs indeed can accommodate single C_{60} molecules. On the MOCN-modified surface shown in Fig. 3a, well-ordered ladder-type networks exist offering two types of elongated cavities (labelled A and B respectively). It is evident that exclusively C_{60} monomers are bound in the offered MOCN host sites, revealing that the MOCN Fe centres cannot effectively bind C_{60}. Moreover, the guests preferentially reside in the larger B-type cavity, and frequently, strings of C_{60} are encountered following the skeleton provided by the ladder-type structure. The smaller type-A cavities cannot hold C_{60} at the given temperature (300 K). This behaviour is associated with the fact that in the larger cavities the fullerenes can interact more effectively with the Cu substrate. The corresponding models shown in Fig. 3b demonstrate that the smaller type-A cavity provides only limited space for C_{60} uptake, whereas the rectangular B cavity is sterically better suited as a host. Type-C Fe-TPA MOCNs cavities may be similarly used to host single C_{60} and keep them apart, as demonstrated by the STM image and the corresponding model in Fig. 3a (inset) and Fig. 3b, respectively. In contrast, on the bare Cu surface left in the area imaged in Fig. 3a, the fullerenes form clusters with hexagonal local order, reflecting effective attractive lateral interfullerene interactions[22].

The STM image in Fig. 4a reveals that C_{60} molecules can also be accommodated in Fe-TMLA MOCNs without altering the network topology. Again, only individual C_{60} monomers are found accommodated in the cavities (a tentative model is given in Fig. 4b),

©2004 Nature Publishing Group

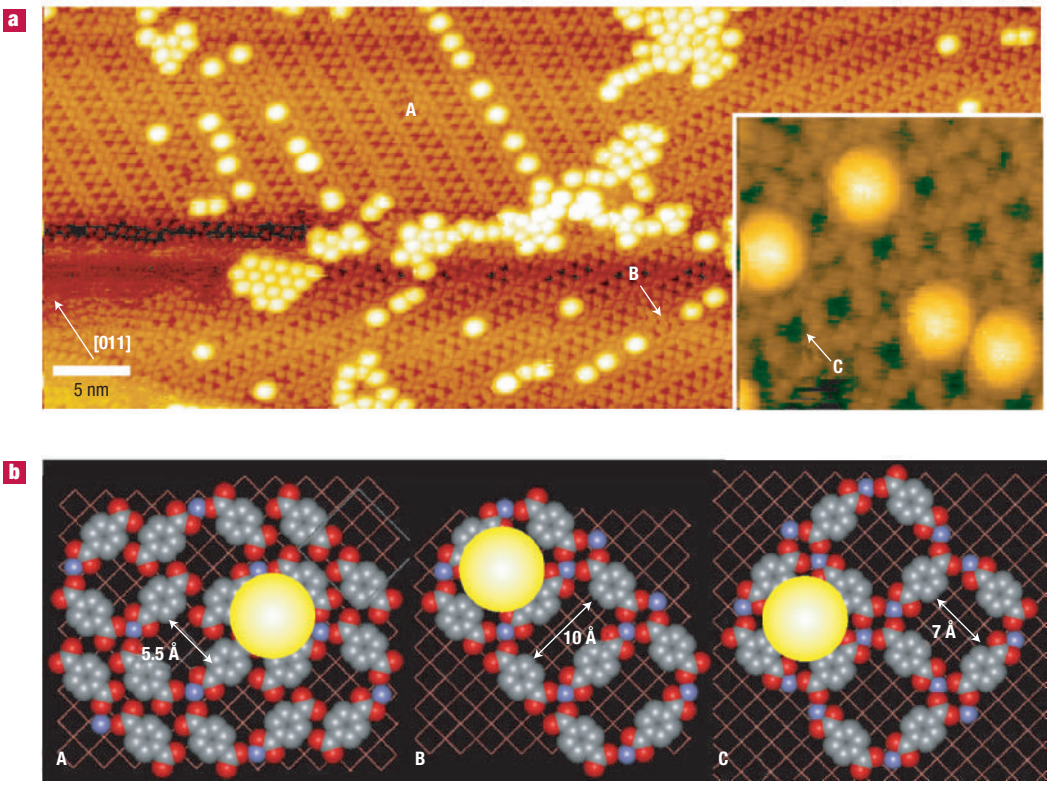

Figure 3 Adsorption of single C_{60} in Fe-TPA host networks. **a**, As seen in the STM image, ladder-type MOCN account for linear arrangements of single C_{60} (yellow spheres) with preferential occupation of larger cavities available (C_{60} clusters are on areas with bare Cu substrate). Inset: C_{60}-monomer accommodation in cavities of type-C network. **b**, Top-view models for C_{60} adsorption in the cavities encountered in **a** with molecules drawn to scale. Possible configurations are labelled in the model and data by A, B and C. In the Van der Waals geometries used for modelling, the molecules appear smaller than in the STM images.

hence the presence of the reactive side groups in the cavities does not alter the adsorption sites. In contrast, with the mesoscale Fe-TDA MOCN cavities, the Cu substrate patches offered are significantly larger than the space occupied by a single C_{60} molecule at the (100) surface. The coadsorption experiments with Fe-TDA networks demonstrate that they remain intact on C_{60} exposure, and thus can be used as a host system. An example is given by the STM image depicted in Fig. 4c, which reveals that single cavities typically host monomers, dimers or trimers of C_{60}. The corresponding model (Fig. 4d) demonstrates that with the accommodation of a C_{60} trimer, most of the available space provided by the cavity is occupied. Accordingly, tetramers were only very rarely observed.

A crucial property of the systems described here is the reversibility and strength of the C_{60}-cavity interactions. Whereas adsorbed C_{60} molecules bond strongly to the pristine Cu(100) substrate and drive the formation of surface reconstructions[22], we may use the tailored MOCNs to control the Co–substrate coupling. Moreover, the robustness of the networks used suggests that the guests may be even released by thermal activation or other processes. To gain insight into this issue, thermal annealing experiments were performed. It was found that C_{60} molecules are ejected from the Fe-TPA cavities when a threshold temperature of 370 K is exceeded. STM measurements taken after annealing revealed that C_{60} molecules have disappeared from the cavities and aggregate in clusters on bare Cu patches where no networks interfere. It is known that the desorption of C_{60} from bare Cu surfaces occurs at significantly higher temperatures (730 K for the case of Cu(110))[23]. The significantly lower temperature detected for the cavity release signals that the C_{60} molecules in the MOCNs interact only weakly with the Cu substrate and the cavity rims. This is associated with the rigidity of the nanopores and the inert chemical nature of the phenyl rings. The corresponding space limitations result in a small contact area and hence a weaker coupling between C_{60} and Cu surface atoms. In contrast, the cavities of the Fe-TDA MOCN are considerably larger than the space occupied by a single C_{60} molecule. Thus C_{60} should be able to bond to the Cu surface more strongly, coming closer to the situation of adsorption at the pristine surface. Indeed, we found that the threshold temperature to release C_{60} adsorbed in Fe-TDA cavities must exceed 500 K, the highest temperature explored in our experiments (MOCNs become unstable for $T > 500$ K).

There is no release of C_{60} molecules from both types of Fe-TMLA cavities up to temperatures as high as 420 K, implying that the host–guest interaction is enhanced here despite the similar host size with regard to the same type of Fe-TPA MOCN cavities. As the C_{60}–Cu gap is similar in both cases, contributions from the C_{60}–substrate interaction are expected to be comparable. The increased bonding strength thus indicates that the additional side group at the TMLA ortho position strongly modifies the chemical properties of the nanocavities. As suggested by Fig. 4b, the cavity rim interferes in the host–guest interactions (we presume that in the course of network formation this group is deprotonated by the reactive Fe adatoms, such that a carboxylate exists). The enhanced accommodation energy is associated with a local contribution from the reactive group at the MOCN rims, which interacts more strongly with C_{60} molecules than the aromatic ring in the case of TPA. The substantial C_{60}–rim interaction strength is

©2004 Nature Publishing Group

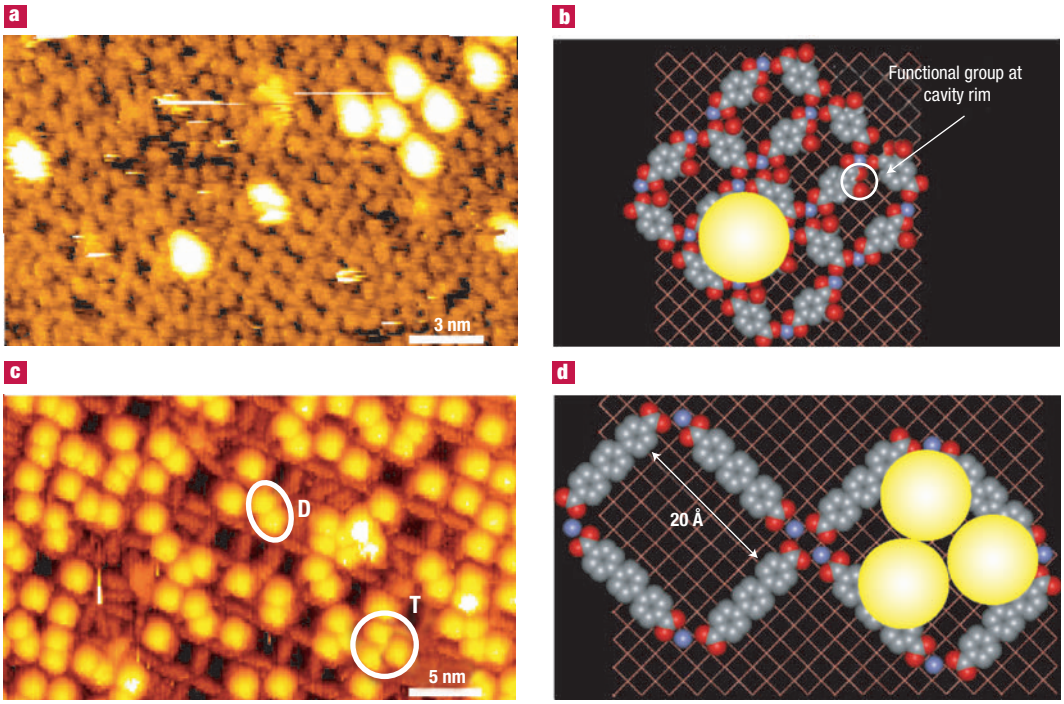

Figure 4 Adsorption of C_{60} in Fe-TMLA and Fe-TDA network hosts. a, Similar to the Fe-TPA networks, Fe-TMLA networks host C_{60} monomers. **b**, Model of accommodation of a C_{60} monomer in Fe-TMLA MOCN cavities. The indicated functional side group at the ortho position, which is supposed to be rotated by 90° out of the molecular plane to avoid too small oxygen-to-oxygen distances, strongly affects the chemical reactivity of the cavity. **c**, The mesoscale cavities in 2D reticulated Fe-TDA networks can host C_{60} monomers, dimers (D) or trimers (T). **d**, Model of rectangular cavity and accommodation of a C_{60} trimer.

further supported by manipulation experiments. Manipulation of individual C_{60} molecules with the STM tip often results in local network disintegration in the case of Fe-TMLA networks, whereas Fe-TPA networks remain intact after undergoing the same operation. Heating up to 450 K leads also to a disintegration of the Fe-TMLA network architecture, that is, the uptake of C_{60} in Fe-TMLA nanocavities is irreversible, which again is associated with the enhanced local reactivity in the vicinity of the molecular side group.

Table 1 summarizes the threshold temperatures for the release of C_{60} guest molecules from the respective surface-supported MOCN cavities. The dominating host–guest interactions for each case, from weak C_{60}–phenyl coupling to strong C_{60}–Cu binding, are indicated.

In conclusion, our findings demonstrate that surface-supported Fe-carboxylate MOCNs with controlled pore size and functionality represent robust templates for the handling and organisation of functional species at the nanoscale. In particular, we demonstrated their aptitude to accommodate C_{60} molecules, whereby the corresponding host–guest interactions can be steered by constructing MOCN architectures with specific topology and functionalized rims. This tuning of the lateral and adsorbate–substrate interactions of included guests is particularly important for selective adsorption or surface chemical reactions. Generally speaking, however, engineering MOCNs at surfaces is expected to provide a versatile rationale towards the fabrication of novel patterned layered materials and templates for positioning nanoscale objects, which may comprise functionalities of interest in a great variety of fields, such as sensing, heterogenous catalysis, nanoelectronics, nanomagnetism, spintronics or molecular magnetism.

Table 1 Threshold temperatures for C_{60} ejection from different MOCN cavities; dominating host–guest interactions expected from modelling for each case are listed.

MOCN type	T_{eject} (K)	Dominant host–guest interaction
TPA (A)	<300	Aromatic ring-to-C_{60}
TPA (B, C)	370	Cu-to-C_{60} (loose-contact)
TMLA	Destructive	Functionalized rim-to-C_{60}
TDA	>500	Cu-to-C_{60}(close-contact)
Cu(110)	730	Cu-to-C_{60}(close-contact)

METHODS

The organic linker molecules and iron atoms were deposited on the metal surface sequentially in a standard ultra-high-vacuum chamber with a base pressure of ~3×10^{-10} mbar. Cu(100) was cleaned by repeated cycles of Ar^+ sputtering and subsequent annealing to 800 K, whereupon flat terraces of up to 50 nm width separated by monatomic steps were obtained. TDA was synthesised following a recipe given elsewhere[24]. To purify the crude TDA, it was converted to the di(acid chloride) compound using thionyl chloride and pyridine. The solution of the di(acid chloride) in boiling benzene was treated with activated carbon and filtered. The di(acid chloride) in the filtrate was recrystallized in benzene, then mixed with Millipore water and refluxed overnight. TDA in powder form was obtained after filtration, and further purified by sublimation three times at about 220 °C and 0.1 mbar. TPA (99+%, Sigma-Aldrich) and TDA were deposited by organic molecular beam epitaxy (OMBE) from Knudsen-cell-type evaporators, held at 440 K (TPA), 415 K (TMLA) and 530 K (TDA) during deposition. Fe atoms were subsequently evaporated using an electron-beam heating evaporator. Samples were annealed after depositions at 450 K for 5 minutes to increase the mobility and reactivity of the adsorbates, and thus obtain well-ordered structures. For the organic precursor layers, coverages below full monolayer saturation were usually used to allow for regular reticulation of the more open network structures. The ratios between the numbers of deposited molecules and Fe atoms are 0.49, 0.8 and 0.52 for TPA MOCNs of type A, B and C, respectively; and 0.4 for TDA MOCN shown in Fig. 2. The fractional Fe coverages thus somewhat exceed the Fe amount required in the networks. This deviation is attributed to the effective loss of Fe atoms in other surface chemical processes such as step decoration, Fe island formation or possibly substrate atom exchange processes. C_{60} molecules were deposited by OMBE with the nanostructured surface held at 300 K. STM experiments using the constant current mode were subsequently performed *in situ* following cool-down to room temperature. To probe the thermal ejection of C_{60} hosts, the system was held for a time interval of 10 minutes at the indicated temperature.

©2004 Nature Publishing Group

Received 17 June 2003; accepted 26 January 2004; published 7 March 2004.

References

1. Davis, M. E. Ordered porous materials for emerging applications. *Nature* **417,** 813–821 (2002).
2. Stein, A. Advances in microporous and mesoporous solids - highlights of recent progress. *Adv. Mater.* **15,** 763–775 (2003).
3. Yaghi, O. M. *et al.* Reticular synthesis and the design of new materials. *Nature* **423,** 705–714 (2003).
4. Fujita, M. Molecular paneling through metal-directed self-assembly. *Struct. Bond.* **96,** 177–201 (2000).
5. Seo, J. S. *et al.* A homochiral metal-organic porous material for enantioselective separation and catalysis. *Nature* **404,** 982–986 (2000).
6. Biradha, K., Hongo, Y. & Fujita, M. Open square-grid coordination polymers of the dimensions 20 × 20 Å: Remarkably stable and crystalline solids even after guest removal. *Angew. Chem. Intl Edn* **39,** 3843–3845 (2000).
7. Eddaoudi, M. *et al.* Modular chemistry: Secondary building units as a basis for the design of highly porous and robust metal-organic carboxylate networks. *Acc. Chem. Res.* **34,** 319–330 (2001).
8. Eddaoudi, M. *et al.* Systematic design of pore size and functionality in isoreticular MOFs and their application in methane storage. *Science* **295,** 469–472 (2002).
9. Rosi, N. R. *et al.* Hydrogen storage in microporous metal-organic frameworks. *Science* **300,** 1127–1129 (2003).
10. Dmitriev, A., Spillmann, H., Lin, N., Barth, J. V. & Kern, K. Modular assembly of two-dimensional metal-organic coordination networks at a metal surface. *Angew. Chem. Intl Edn* **42,** 2670–2673 (2003).
11. Chui, S. S.-Y., Lo, S. M.-F., Charmant, J. P. H., Orpen, A. G. & Williams, I. D. A chemically functionalizable nanoporous material $[Cu_3(TMA)_2(H_2O)_3]_n$. *Science* **283,** 1148–1150 (1999).
12. Mori, W. & Takamizawa, S. Microporous materials of metal carboxylates. *J. Sol. Chem.* **152,** 120–129 (2000).
13. Moulton, B., Lu, J., Hajndl, R., Hariharan, S. & Zaworotko, M. J. Crystal engineering of a nanoscale Kagomé lattice. *Angew. Chem. Intl Edn* **41,** 2821–2824 (2002).
14. Maspoch, D. *et al.* A nanoporous molecular magnet with reversible solvent-induced mechanical and magnetic properties. *Nature Mater.* **2,** 190–195 (2003).
15. Lin, N., Dmitriev, A., Weckesser, J., Barth, J. V. & Kern, K. Real-time single-molecule imaging of the formation and dynamics of coordination compounds. *Angew. Chem. Intl Edn* **41,** 4779–4783 (2002).
16. Messina, P. *et al.* Direct observation of chiral metal-organic complexes assembled on a Cu(100) surface. *J. Am. Chem. Soc.* **124,** 14000–14001 (2002).
17. Lingenfelder, M. *et al.* Towards surface-supported supramolecular architectures: Tailored coordination assembly of 1,4-benezendicarboxylate and Fe on Cu(100). *Chem. Eur. J.* (in the press).
18. Theobald, J. A., Oxtoby, N. S., Phillips, M. A., Champness, N. R. & Beton, P. H. Controlling molecular deposition and layer structure with supramolecular surface assemblies. *Nature* **424,** 1029–1031 (2003).
19. Rudolf, P. in *Proceedings of the International Winterschool on Electronic Properties of Novel Materials. Fullerenes and Fullerene Nanostructures* (eds Kuzmany, H., Fink, J., Mehring, M. & Roth, S.)263–275 (World Scientific, Singapore, 1996).
20. Hamza, A. V. in *Fullerenes: Chemistry, Physics and Technology* (eds Kadish, K. M. & Ruoff, R. S.) 531–554 (Wiley, New York, 2000).
21. Lee, K., Song, H. & Park, J. T. [60]Fullerene - metal cluster complexes: novel bonding modes and electronic communication. *Acc. Chem. Res.* **36,** 78–86 (2003).
22. Abel, M. *et al.* Scanning tunneling microscopy and x-ray photoelectron diffraction investigation of C_{60} films on Cu(100). *Phys. Rev. B* **67,** 245407 (2003).
23. Fasel, R., Agostino, R. G., Aebi, P. & Schlapbach, L., Unusual molecular orientation and frozen librational motion of C_{60} on Cu(110). *Phys. Rev. B.* **60,** 4517–4520 (1999).
24. Campbell, T. W. Dicarboxylation of terphenyl. *J. Am. Chem. Soc.* **82,** 3126–3128 (1962).

Correspondence and requests for materials should be addressed to N.L.

Competing financial interests

The authors declare that they have no competing financial interests.

©2004 Nature Publishing Group